

# MEMORY FORCING: SPATIO-TEMPORAL MEMORY FOR CONSISTENT SCENE GENERATION ON MINECRAFT

006 **Anonymous authors**

007 Paper under double-blind review

## ABSTRACT

Autoregressive video diffusion models have proved effective for world modeling and interactive scene generation, with Minecraft gameplay as a representative application. To faithfully simulate play, a model must generate natural content while exploring new scenes and preserve spatial consistency when revisiting explored areas. Under limited computation budgets, it must compress and exploit historical cues within a finite context window, which exposes a trade-off: Temporal-only memory lacks long-term spatial consistency, whereas adding spatial memory strengthens consistency but may degrade new scene generation quality when the model over-relies on insufficient spatial context. We present *Memory Forcing*, a learning framework that pairs training protocols with a geometry-indexed spatial memory. *Hybrid Training* exposes distinct gameplay regimes, guiding the model to rely on temporal memory during exploration and incorporate spatial memory for revisits. *Chained Forward Training* extends autoregressive training with model rollouts, where chained predictions create larger pose variations and encourage reliance on spatial memory for maintaining consistency. *Point-to-Frame Retrieval* efficiently retrieves history by mapping currently visible points to their source frames, while *Incremental 3D Reconstruction* maintains and updates an explicit 3D cache. Extensive experiments demonstrate that Memory Forcing achieves superior long-term spatial consistency and generative quality across diverse environments, while maintaining computational efficiency for extended sequences.

## 1 INTRODUCTION

Autoregressive video models (Bar et al., 2025; Chen et al., 2024; Song et al., 2025) based on diffusion (Ho et al., 2020; Dhariwal & Nichol, 2021; Peebles & Xie, 2023) have recently emerged as powerful tools for world modeling, showing strong capabilities in interactive scene generation (Feng et al., 2024; Parker-Holder et al., 2024), particularly in open-world environments like Minecraft, where multi-dimensional controls enable rich user interactions. These models (Decart et al., 2024; Guo et al., 2025; Cheng et al., 2025) learn to predict future frames conditioned on past observations and user actions, enabling autoregressive (AR) rollouts that react to player inputs in real time. Within the AR paradigm, the model must condition on a context window of past frames, but latency and memory limits bound the window size. Therefore, it is critical to compress and prioritize historical information (*i.e.*, memory) within this limited window.

In prior works, the allocation of memory manifests in two characteristic failure modes, as shown in Fig. 1. Models that incorporate long-term spatial memory preserve consistency on revisits (Fig. 1(a)) but fail in novel scenes exploration. Conversely, temporal-only models fail to maintain spatial consistency upon revisit (Fig. 1(b)). Moreover, teacher-forced training Huang et al. (2025) underestimates inference-time drift, encouraging over-reliance on short-horizon temporal cues and underuse of retrieved memory at test time. These observations motivate a training framework that enables the model to modulate its reliance on temporal and spatial memory across exploration and revisit regimes, thereby balancing exploration flexibility and revisit consistency.

To address these limitations, we introduce Memory Forcing, a training framework that forces the model to flexibly and effectively use temporal and spatial memory under a fixed window. Specifi-

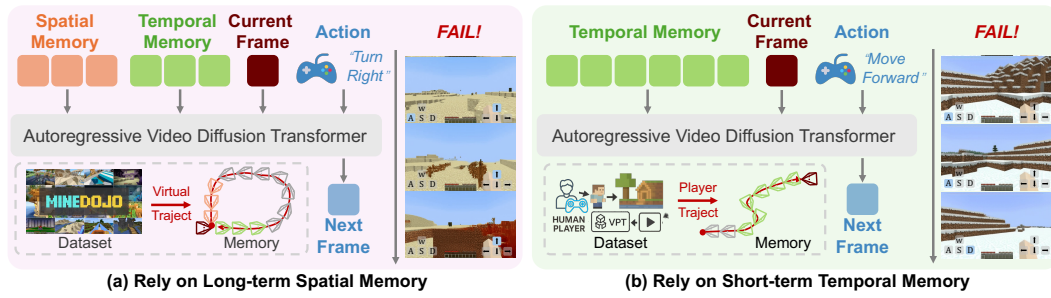


Figure 1: Two paradigms of autoregressive video models and their fail cases. (a) Long-term spatial memory models maintain consistency when revisiting areas yet deteriorate in new environments. (b) Temporal memory models excel in new scenes yet lack spatial consistency when revisiting areas.

Hybrid Training uses distinct data distributions to emulate complementary gameplay regimes, so the model learns to rely on temporal memory for novel-scene exploration and to incorporate spatial memory on revisits for consistency. In practice, we adopt temporal-only conditioning on VPT (Baker et al., 2022) (human play, exploration-oriented) and spatial&temporal conditioning on MineDojo (Fan et al., 2022) (simulated trajectories with frequent revisits and adjacent viewpoints), achieving a balanced optimum across the two tasks. Besides, we introduce Chained Forward Training to augment autoregressive learning with model rollouts: it progressively replaces ground-truth temporal context with the model’s own predictions, amplifies pose/viewpoint drift across windows, and thus encourages reliance on spatial memory to maintain revisit consistency.

Beyond the training protocol, we equip the model with Geometry-indexed Spatial Memory. Prior frame-level retrieval (Xiao et al., 2025; Chen et al., 2025) is appearance-based, sensitive to viewpoint and illumination changes, and prone to accumulating near-duplicate views under neighboring poses. As sequences grow, redundancy and lookup latency grow with the size of the memory bank. State-space methods (Po et al., 2025) compress history into latent states and alleviate this efficiency issue, but they lack explicit spatial indexing, making it difficult to specify which spatial evidence to retain and which redundancy to discard. Instead, we maintain a coarse scene representation via streaming 3D reconstruction and retrieve history with point-to-frame mapping: currently visible 3D points are back-traced to their source frames to select a compact, pose-relevant set of views. This geometry-anchored access is robust to viewpoint changes, bounds the candidate set (top- $k$ ), and scales with visible spatial coverage rather than sequence length.

We conduct comprehensive experiments on Minecraft benchmark (Fan et al., 2022) across three critical dimensions: long-term memory with spatial revisitations, generalization on unseen terrains, and generation in new environments. Our method achieves superior performance across all three settings compared to both temporal-only and spatial memory baselines, while our Geometry-indexed Spatial Memory demonstrates 7.3x faster retrieval speed with 98.2% less memory storage. These results demonstrate that Memory Forcing effectively resolves the trade-off between spatial consistency and generative quality while maintaining computational efficiency.

In summary, our contributions are threefold:

- We introduce Memory Forcing, a framework that simultaneously addresses capability trade-offs and efficiency limitations in memory-augmented video generation.
- We develop the Hybrid Training and Chained Forward Training strategy that teaches models to use temporal memory for exploration and incorporate spatial memory for revisits, and a Geometry-indexed Spatial Memory built via streaming 3D reconstruction with Point-to-Frame Retrieval, whose lookup cost scales with visible spatial coverage rather than sequence length.
- Extensive experiments demonstrate that Memory Forcing achieves superior performance in both spatial consistency and generative quality in new environments, while maintaining computational efficiency for extended sequences.

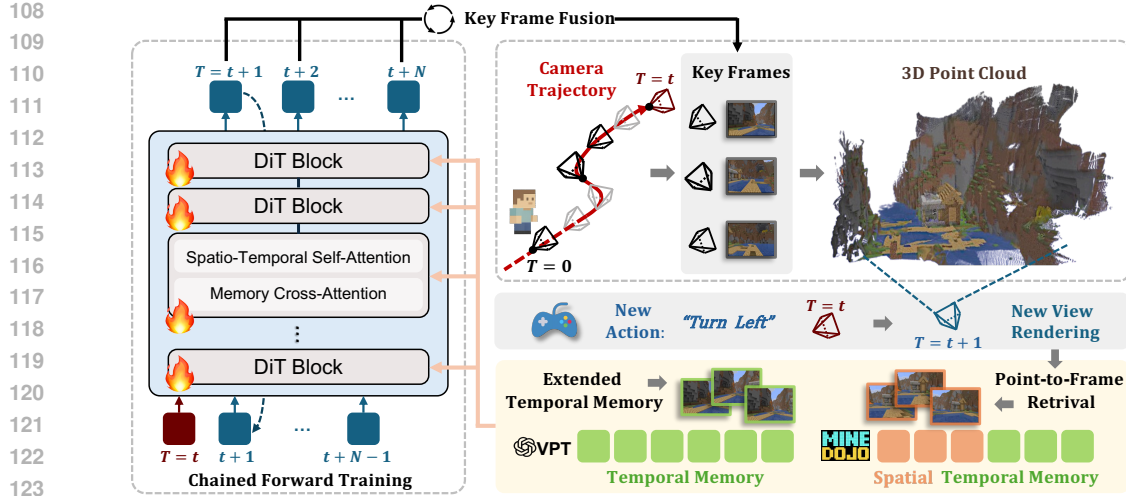


Figure 2: Memory Forcing Pipeline. Our framework combines spatial and temporal memory for video generation. 3D geometry is maintained through streaming reconstruction of key frames along the camera trajectory. During generation, Point-to-Frame Retrieval maps spatial context to historical frames, which are integrated with temporal memory and injected together via memory cross-attention in the DiT backbone. Chained Forward Training creates larger pose variations, encouraging the model to effectively utilize spatial memory for maintaining long-term geometric consistency.

## 2 RELATED WORKS

**Autoregressive Video Models.** Autoregressive video generation (Harvey et al., 2022; Li et al., 2025b; Xie et al., 2025; Wu et al., 2024; Teng et al., 2025; Henschel et al., 2025) enables long video synthesis by conditioning on preceding frames. Early token-based approaches (Wu et al., 2024; Kondratyuk et al., 2023) achieved temporal consistency but compromised visual fidelity. Recent diffusion-based methods (Voleti et al., 2022; Hong et al., 2024; Chen et al., 2024; Song et al., 2025) achieve superior quality through masked conditioning and per-frame noise control.

**Interactive Game World Model.** World models predict future states from current states and actions (Ha & Schmidhuber, 2018a;b; Hafner et al., 2019; 2020). Recent video generation advances have enabled interactive world models (OpenAI, 2024; Feng et al., 2024; Parker-Holder et al., 2024; Valevski et al., 2024; Zhang et al., 2025; He et al., 2025; Yu et al., 2025b; Che et al., 2024) for complex gaming environments. Minecraft’s rich action space and environmental dynamics have inspired numerous game world models (Decart et al., 2024; Guo et al., 2025; Cheng et al., 2025; Po et al., 2025; Chen et al., 2025; Xiao et al., 2025). While models like MineWorld (Guo et al., 2025) and NFD (Cheng et al., 2025) show strong interactive capabilities, they lack long-term memory. State-space approaches (Po et al., 2025) introduce memory mechanisms but remain limited by training context length. WorldMem (Xiao et al., 2025) uses pose-based retrieval for long-term memory but suffers from limited novel scene generation and lacks real-time interactivity.

**3D Reconstruction and Memory Retrieval.** Learning-based 3D reconstruction was pioneered by DUST3R (Wang et al., 2024), with subsequent multi-view extensions (Wang et al., 2025a;c; Yang et al., 2025) and streaming methods (Wang et al., 2025b; Wu et al., 2025) for sequential processing. SLAM-based approaches like VGGT-SLAM (Maggio et al., 2025) handle long sequences through incremental submap alignment. For memory retrieval in video generation, existing approaches range from pose-based methods (Xiao et al., 2025; Yu et al., 2025a) using field-of-view overlap to 3D geometry-based approaches like VMem (Li et al., 2025a) with surfel-indexed view selection.

## 3 MEMORY FORCING

We introduce Memory Forcing, a learning framework that pairs training protocols with geometry-indexed spatial memory to enable long-term spatial consistency. Our approach addresses the funda-

162 mental trade-off between temporal memory for generation and spatial memory for revisits through  
 163 Hybrid Training and Chained Forward Training (CFT). Section 3.1 provides background on autore-  
 164 gressive video diffusion models and interactive game world modeling. Section 3.2 presents our  
 165 memory-augmented model architecture. Section 3.3 details our Memory Forcing training protocols.  
 166 Section 3.4 introduces our explicit 3D memory maintenance and retrieval approach.  
 167

### 168 3.1 PRELIMINARIES

170 **Autoregressive Video Diffusion Models.** Autoregressive Video Diffusion Models generate video  
 171 sequences by predicting future frames conditioned on past observations. Following Diffusion For-  
 172 cing (Chen et al., 2024), we denote a video sequence as  $X^{1:T} = x_1, x_2, \dots, x_T$  where each frame  $x_t$   
 173 is assigned an independent noise level  $k_t \in [0, 1]$ . The model learns to predict noise  $\epsilon_\theta(\tilde{X}^{1:T}, k^{1:T})$   
 174 where  $\tilde{X}^{1:T}$  represents the noisy sequence and  $k^{1:T} = k_1, k_2, \dots, k_T$  are the noise levels. The  
 175 training objective minimizes:

$$176 \mathcal{L} = \mathbb{E}_{k^{1:T}, X^{1:T}, \epsilon^{1:T}} \left[ |\epsilon^{1:T} - \epsilon_\theta(\tilde{X}^{1:T}, k^{1:T})|^2 \right] \quad (1)$$

178 This framework enables flexible conditioning patterns for autoregressive generation by allowing  
 179 arbitrary combinations of clean and noisy frames within a sequence.  
 180

181 **Interactive Game World Model.** Interactive game environments present unique challenges for  
 182 video generation models. Players navigate complex 3D environments where actions  $A^{1:T}$  include  
 183 movement commands, camera rotations, and object interactions that directly influence both imme-  
 184 diate visual changes and long-term environment state evolution. For action-conditioned generation,  
 185 the model predicts noise conditioned on both visual observations and actions:  $\epsilon_\theta(\tilde{X}^{1:T}, k^{1:T}, A^{1:T})$   
 186 enabling the model to generate coherent video sequences that respond appropriately to player inputs.  
 187

### 188 3.2 MEMORY-AUGMENTED ARCHITECTURE

189 We follow previous works (Cheng et al., 2025) in adopting block-wise causal attention for efficient  
 190 spatio-temporal modeling, adaLN-zero conditioning for action integration, and 3D positional em-  
 191 beddings within a Diffusion Transformer (DiT) backbone. To incorporate long-term spatial memory  
 192 into the generation process, we introduce several memory-specific components.  
 193

194 **Spatial Memory Extraction.** We employ the VGGT (Wang et al., 2025a) network with our cross-  
 195 window scale alignment to enable streaming reconstruction. Historical frames are then efficiently  
 196 extracted through Point-to-Frame Retrieval, providing accurate access to long-term spatial memory.

197 **Memory Cross-Attention.** We integrate Cross-Attention modules within each DiT block to lever-  
 198 age long-term spatial memory during generation. Retrieved historical frames serve as keys and  
 199 values, while current frame tokens act as queries:

$$200 \text{Attention}(\tilde{Q}, \tilde{K}_{\text{spatial}}, V_{\text{spatial}}) = \text{Softmax} \left( \frac{\tilde{Q} \tilde{K}_{\text{spatial}}^T}{\sqrt{d}} \right) V_{\text{spatial}} \quad (2)$$

203 where  $\tilde{Q}$  and  $\tilde{K}_{\text{spatial}}$  are queries and keys augmented with Plücker coordinates to encode relative  
 204 pose information between current and historical viewpoints.  
 205

### 207 3.3 AUTOREGRESSIVE DIFFUSION TRAINING WITH MEMORY FORCING

209 Memory-augmented video generation models face a fundamental capability trade-off. Models relying  
 210 heavily on long-term spatial memory generate content consistent with previously visited scenes,  
 211 but degrade when generating new scenes due to insufficient relevant spatial memory. We therefore  
 212 propose Memory Forcing training protocols that teaches models to dynamically balance these two  
 213 capabilities, learning when to rely on temporal context versus spatial memory.

214 **Hybrid Training.** Our hybrid training approach operates within a fixed context window of  $L$  frames.  
 215 We strategically allocate half the window ( $L/2$  frames) as fixed temporal context frames, while the  
 remaining  $L/2$  frames are flexibly assigned based on the scene context. The complete context

216 window construction can be formalized as:

$$217 \quad \mathcal{W} = [\mathcal{T}_{\text{fixed}}, \mathcal{M}_{\text{context}}] = \begin{cases} [\mathcal{T}_{\text{fixed}}, \mathcal{M}_{\text{spatial}}] & \text{if revisiting previously observed areas} \\ [\mathcal{T}_{\text{fixed}}, \mathcal{T}_{\text{extended}}] & \text{if exploring new scenes} \end{cases} \quad (3)$$

220 where  $\mathcal{T}_{\text{fixed}}$  represents the fixed  $L/2$  recent temporal context frames,  $\mathcal{M}_{\text{spatial}}$  represents long-term  
221 spatial memory retrieved by our Geometry-indexed Spatial Memory 3.4, and  $\mathcal{T}_{\text{extended}}$  represents  
222 additional temporal frames from earlier time steps. This dynamic allocation enables the model to  
223 leverage the most appropriate memory source for each generation scenario.

224 Inspired by Figure 1, we apply different memory strategies to different datasets: spatial memory for  
225 synthetic dataset (Fan et al., 2022) with frequent area revisiting, and extended temporal context for  
226 VPT dataset (Baker et al., 2022) with new scene generation.

227 **Chained Forward Training.** We introduce Chained Forward Training (CFT) to enhance our hybrid  
228 training strategy. CFT sequentially processes temporal windows where predicted frames from earlier  
229 windows are incorporated into subsequent windows, creating cascading dependencies across the  
230 sequence. Details are shown in Algorithm 1 in the Appendix. At each step  $j$ , the temporal window  
231  $\mathcal{W}_j$  contains both ground-truth frames  $\mathbf{x}_k$  and previously predicted frames  $\hat{\mathbf{x}}_k$ , leading to the loss:

$$232 \quad \mathcal{L}_{\text{chain}} = \frac{1}{T} \sum_{j=0}^{T-1} \mathbb{E}_{t, \epsilon} [\|\epsilon - \epsilon_{\theta}(\mathcal{W}_j(\mathbf{x}, \hat{\mathbf{x}}), \mathcal{C}_j, t)\|^2], \quad t \sim \text{Uniform}(0, T_{\text{noise}}), \epsilon \sim \mathcal{N}(0, \mathbf{I}) \quad (4)$$

235 This approach extends autoregressive training with model rollouts, where larger pose variations  
236 created by chained predictions cause inaccuracies to propagate from earlier windows, encouraging  
237 the model to rely on spatial memory for maintaining consistency across revisited areas. Additionally,  
238 by replacing ground truth temporal context with the model’s own predictions during training, this  
239 approach helps reduce accumulation errors that typically arise during autoregressive inference.

#### 240 3.4 GEOMETRY-INDEXED SPATIAL MEMORY

242 Our Geometry-indexed Spatial Memory maintains explicit scene geometry and enables efficient  
243 retrieval of long-term historical visual information based on 3D spatial relationships. This approach  
244 consists of two key components: Point-to-Frame Retrieval for identifying relevant historical frames  
245 and Incremental 3D Reconstruction for maintaining and updating scene representations.

247 **Point-to-Frame Retrieval.** For each current frame, we project the global point cloud to the current  
248 camera pose and analyze the source frame indices of visible points to identify the most relevant  
249 historical frames:

$$250 \quad \mathcal{H}_t = \arg \max_{k=1, \dots, 8} \text{Count}(\text{source}(p_i) : p_i \in \mathcal{P}_{\text{visible}}^t) \quad (5)$$

251 where  $\mathcal{P}_{\text{visible}}^t$  represents the set of points visible under the current camera pose for frame  $t$ ,  
252  $\text{source}(p_i)$  denotes the source frame index of point  $p_i$ , and  $\mathcal{H}_t$  contains the top-8 most frequently  
253 referenced historical frames among the visible points. This retrieval mechanism maintains  $O(1)$   
254 complexity regardless of sequence length, enabling scalable processing.

255 **Incremental 3D Reconstruction.** We adopt a selective reconstruction approach that dynamically  
256 determines keyframes based on spatial information content. A frame qualifies as a keyframe when  
257 it either reveals previously unobserved regions or when insufficient historical context exists:

$$258 \quad \text{IsKeyframe}(t) = \mathcal{C}(I_t^{\text{proj}}) \vee (|\mathcal{H}_t| < \tau_{\text{hist}}) \quad (6)$$

260 where  $\mathcal{C}(I_t^{\text{proj}})$  determines whether the current view contributes new spatial coverage when projected  
261 onto existing geometry, and  $\tau_{\text{hist}} = 8$  serves as the minimum historical frame count threshold.

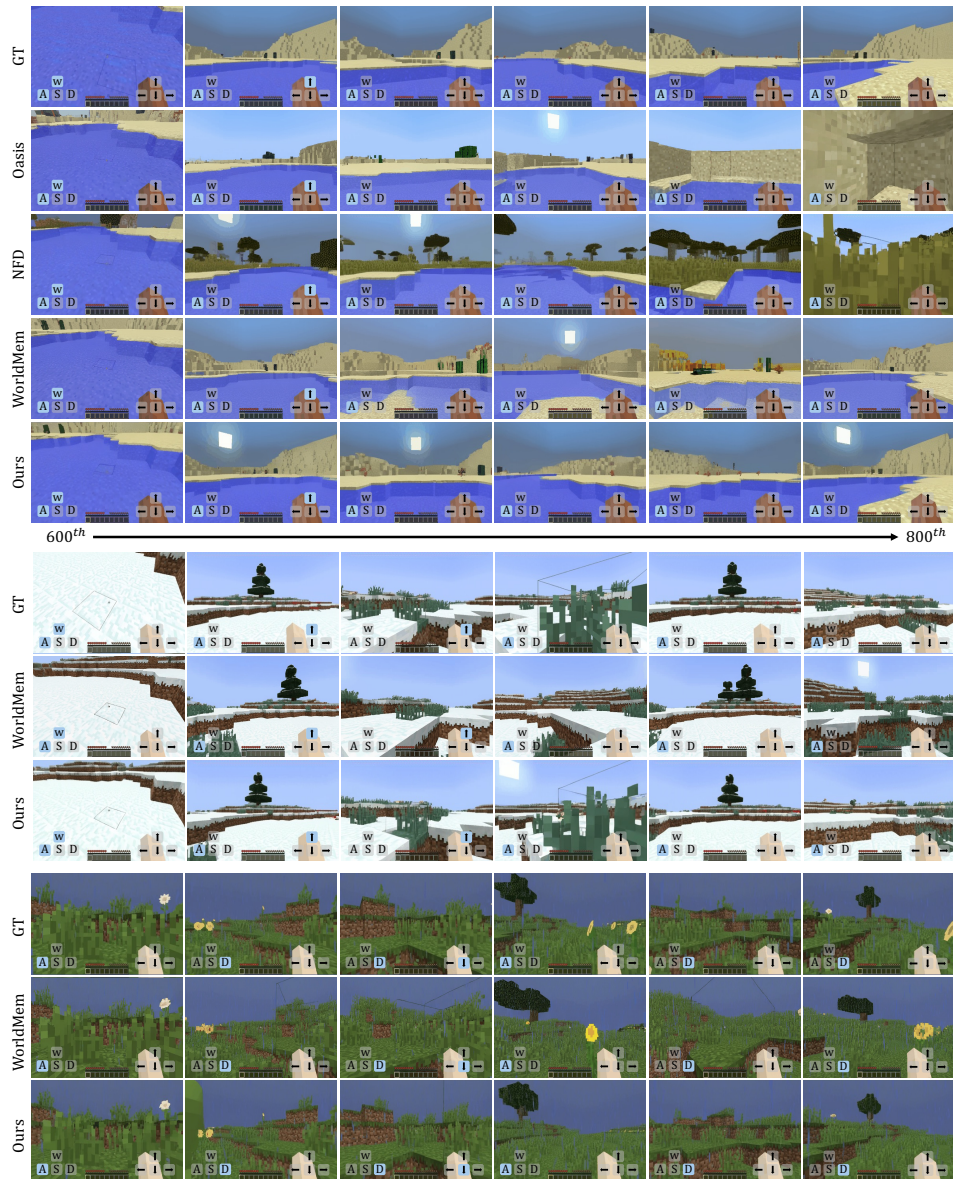
262 Upon reaching window capacity, we jointly process keyframes, historical frames selected via Point-  
263 to-Frame Retrieval for improved geometric consistency, and overlapping frames from the previous  
264 window that provide depth scale reference for aligning the new window. VGGT generates  
265 relative depth maps and confidence scores for each frame in this window, followed by our cross-  
266 window scale alignment module that establishes consistent depth scale across windows through  
267 correspondence analysis in overlapping regions. 3D geometry is reconstructed through depth map  
268 back-projection using camera extrinsics derived from quaternion-composed poses:

$$269 \quad \mathbf{E} = \begin{bmatrix} \mathbf{R}(\text{pitch}, \text{yaw}) & -\mathbf{R}\mathbf{C} \\ \mathbf{0}^T & 1 \end{bmatrix} \quad (7)$$

270 where  $\mathbf{R}(pitch, yaw)$  encodes the viewing orientation through quaternion-based rotation composition,  
 271 and  $\mathbf{C} = [x, y, z]^T$  specifies the camera’s spatial position. The reconstructed geometry is  
 272 subsequently integrated into our global representation through spatially-aware voxel sampling.  
 273

274 This design achieves efficient scene representation and retrieval through two key mechanisms. First,  
 275 selective keyframe reconstruction processes and stores only frames that contribute new spatial cov-  
 276 erage, preventing redundant computation and storage when revisiting encountered areas. Second,  
 277 voxel downsampling maintains an upper bound on point density for any pose region, ensuring con-  
 278 stant retrieval complexity regardless of temporal sequence length or scene scope. These mechanisms  
 279 collectively ensure that memory consumption scales with spatial coverage rather than temporal du-  
 280 ration, enabling efficient processing of extended sequences.

## 281 4 EXPERIMENTS



322 Figure 3: Memory capability comparison across different models for maintaining spatial consistency  
 323 and scene coherence when revisiting previously observed areas.

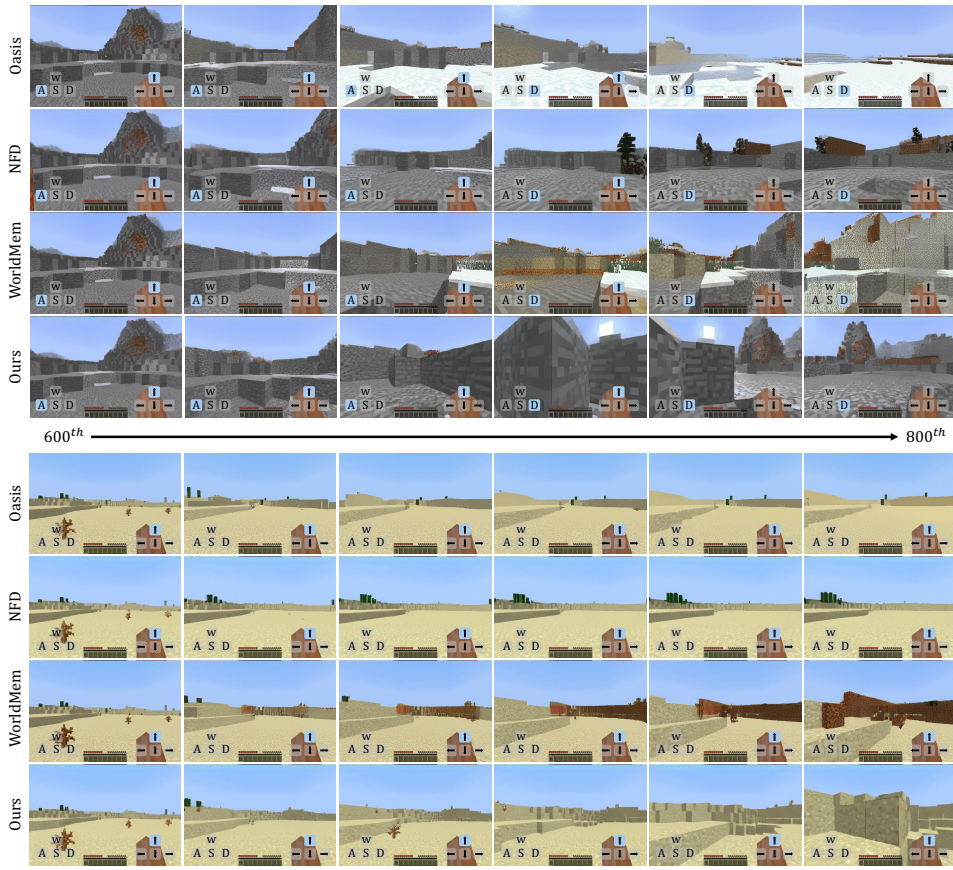


Figure 4: Generalization performance on unseen terrain types (top) and generation performance in new environments without historical spatial memory (bottom) across different models.

We conduct comprehensive experiments to evaluate our Memory Forcing framework through both quantitative and qualitative analyses. We demonstrate our model’s long-term memory capabilities, generalization, and generation performance in new environments on our constructed Minecraft benchmark, and assess the retrieval and storage efficiency of our Geometry-indexed Spatial Memory. Additionally, we provide ablation studies on our frame retrieval strategy and training methodology.

#### 4.1 EXPERIMENTAL SETUP

**Implementation Details.** Our model converges after approximately 400k training steps across 24 GPUs with batch size of 4. We employ the Adam optimizer with a learning rate of 4e-5. All training and evaluation are conducted on NVIDIA H20/H100 GPUs using PyTorch. We employ a 2D variational autoencoder following NFD (Cheng et al., 2025) for frame tokenization, providing 16 $\times$  spatial compression and transforming each frame into 24  $\times$  14 continuous tokens. Video frames are resized to 384  $\times$  224 resolution, maintaining the original aspect ratio and sufficient visual detail.

**Baselines.** We compare our approach against baseline models including Oasis (Decart et al., 2024) and NFD (Cheng et al., 2025), as well as the long-term memory model WorldMem (Xiao et al., 2025). For fair comparison, all models use a 16-frame context window during both training and evaluation. All models follow their respective training configurations and are trained on identical Synthetic datasets for approximately 500-600k steps to ensure consistent evaluation conditions.

**Datasets.** For training, we use the VPT (Baker et al., 2022) dataset, which pairs 25-dimensional action vectors with corresponding video sequences. Following previous work (Guo et al., 2025), we exclude frames without actions or when the graphical user interface is visible to reduce noise. Additionally, we utilize a synthetic dataset generated from MineDoJo (Fan et al., 2022) for long-term memory training, following the configuration of WorldMem (Xiao et al., 2025), which consists

378	379	Method	380				381				382			
			FVD ↓	PSNR ↑	SSIM ↑	LPIPS ↓	FVD ↓	PSNR ↑	SSIM ↑	LPIPS ↓	FVD ↓	PSNR ↑	SSIM ↑	LPIPS ↓
Oasis	196.8	16.83	0.5654	0.3791	477.3	14.74	0.5175	0.5122	285.7	14.51	0.5063	0.4704		
NFD	220.8	16.35	0.5819	0.3891	442.6	15.49	0.5564	0.4638	349.6	14.64	0.5417	0.4343		
WorldMem	122.2	19.32	0.5983	0.2769	328.3	16.23	0.5178	0.4336	290.8	14.71	0.4906	0.4531		
Ours	<b>84.9</b>	<b>21.41</b>	<b>0.6692</b>	<b>0.2156</b>	<b>253.7</b>	<b>19.86</b>	<b>0.6341</b>	<b>0.2896</b>	<b>185.9</b>	<b>17.99</b>	<b>0.6155</b>	<b>0.3031</b>		

383 Table 1: A comparison of different methods across various capabilities and evaluation metrics.  
384

385	386	387	Frame Range	388		389		390		391		392	
				Speed	Mem.	Speed	Mem.	Speed	Mem.	Speed	Mem.	Speed	Mem.
WorldMem	10.11	+1000	3.43	+1000	2.06	+1000	1.47	+1000	4.27	4000			
Ours	<b>18.57</b>	<b>+25.45</b>	<b>27.08</b>	<b>+19.70</b>	<b>41.36</b>	<b>+14.55</b>	<b>37.84</b>	<b>+12.95</b>	<b>31.21</b>	<b>72.65</b>			

393 Table 2: Comparison of retrieval efficiency between WorldMem and our Geometry-indexed Spatial  
394 Memory across different sequence lengths. “Mem.” denotes the number of frames in memory bank.  
395

396 of 11k videos containing 1,500-frame action sequences with frequent pose transitions to previously  
397 visited spatial locations. For evaluation, we constructed three datasets using MineDojo to assess the  
398 model’s performance across various aspects:

- 399 • **Long-term Memory:** 150 long video sequences (1,500 frames) were isolated from the World-  
400 Mem dataset (Xiao et al., 2025) to evaluate the model’s capacity for long-term memory retention.
- 401 • **Generalization Performance:** We constructed 150 video sequences (800 frames) from nine un-  
402 seen Minecraft terrains using MineDojo (Fan et al., 2022) to evaluate the model’s generalization.
- 403 • **Generation Performance:** We constructed 300 video sequences (800 frames) using Mine-  
404 Dojo (Fan et al., 2022) to assess generation performance in new environments.

405 **Evaluation Metrics.** We evaluate our model’s performance using established video quality met-  
406 rics. We measure perceptual quality with Fréchet Video Distance (FVD) and Learned Perceptual  
407 Image Patch Similarity (LPIPS), while assessing pixel-level accuracy through Peak Signal-to-Noise  
408 Ratio (PSNR) and Structural Similarity Index Measure (SSIM). These metrics collectively provide  
409 comprehensive assessment of both visual fidelity and consistency in generated sequences.

## 410 4.2 MODEL CAPABILITIES ASSESSMENT

411 For all quantitative and qualitative evaluations, we generate frames 600-800 (200 frames) to assess  
412 long-sequence generation capabilities using the datasets described in our experimental setup.

413 **Long-term Memory.** We evaluate models’ ability to maintain spatial consistency and scene coher-  
414 ence when revisiting previously observed areas using our long-term memory evaluation dataset. As  
415 demonstrated in Table 1, our method achieves superior performance across all metrics, indicating  
416 enhanced visual fidelity in long-sequence generation. Figure 3 further shows that our model demon-  
417 strates the most precise memory when returning to previously visited locations. While WorldMem  
418 exhibits some memory retention capabilities, it produces inaccurate and unstable view generation  
419 with visual artifacts in the generated scenes (e.g., the fifth frame in the fourth row). In contrast, the  
420 remaining baseline models lack long-term memory mechanisms, resulting in spatial inconsistencies  
421 where camera viewpoint changes inappropriately alter scene geometry and terrain features.

422 **Generalization Performance.** Using our generalization evaluation dataset with nine novel terrain  
423 scenarios, our approach demonstrates robust generalization performance, significantly outperforming  
424 baselines across all metrics as shown in Table 1, indicating strong adaptability to unseen envi-  
425 ronments. The top portion of Figure 4 illustrates qualitative generalization results, where our model  
426 generates stable and consistent outputs across novel terrains. In contrast, WorldMem and NFD ex-  
427 hibit artifacts in their generations, while Oasis shows scene inconsistencies.

428 **Generation Performance.** Our comprehensive evaluation using the generation performance dataset  
429 demonstrates that our method outperforms all baselines across metrics in Table 1, highlighting the  
430 effectiveness of balancing long-term and temporal memory. The bottom portion of Figure 4 illus-  
431 trates generation performance in new environments, where our model exhibits responsive movement  
432 dynamics with distant scenes progressively becoming clearer as the agent approaches. In contrast,

	Training Strategies			Retrieval Strategies		Metrics			
	FT	HT-w/o-CFT	MF	Pose-based	3D-based	FVD ↓	PSNR ↑	SSIM ↑	LPIPS ↓
✓	✓			✓	✓	366.1	15.09	0.5649	0.4122
		✓		✓	✓	230.4	16.24	0.5789	0.3598
			✓	✓	✓	225.9	16.24	0.5945	0.3722
					✓	<b>165.9</b>	<b>18.17</b>	<b>0.6222</b>	<b>0.2876</b>

Table 3: Ablation study comparing training strategies and retrieval mechanisms. FT: full-parameter fine-tuning, HT-w/o-CFT: hybrid training without CFT, MF: Memory Forcing with HT and CFT.

WorldMem experiences significant quality degradation in this scenario, NFD shows minimal variation in distant scenes regardless of agent movement, and Oasis generates oversimplified distant scenes that lack proper distance-based visual transitions.

### 4.3 EFFICIENCY OF GEOMETRY-INDEXED SPATIAL MEMORY

Table 2 evaluates the computational efficiency and storage requirements of our Geometry-indexed Spatial Memory compared to WorldMem’s retrieval approach across 20 4000-frame MineDojo videos. While WorldMem stores all historical frames and performs linear-complexity retrieval across the entire collection, our selective keyframe approach reduces memory bank size by 98.2% while achieving 7.3x faster retrieval speed at 0-3999 frames. Efficiency gains increase with sequence length, reaching 25.7x speedup in the 3000-3999 frame range as WorldMem becomes increasingly slower. WorldMem’s memory bank grows linearly with sequence length, while our Geometry-indexed Spatial Memory scales with spatial coverage expansion, storing only keyframes with new geometric information. Our speeds include the complete 3D memory pipeline (reconstruction and retrieval), while WorldMem’s include pose-based retrieval across all stored frames.

### 4.4 ABLATION STUDIES

Table 3 shows ablation studies on 300 videos from Long-term Memory and Generation Performance datasets analyzing the contributions of our training strategies and retrieval mechanisms.

**Training Strategy Analysis.** We compare three training approaches: full-parameter Fine-Tuning (FT) after VPT pre-training, Hybrid Training without Chained Forward Training (HT-w/o-CFT), and our complete Memory Forcing training strategy (MF). Direct fine-tuning achieves limited performance as the model struggles to balance temporal memory and spatial memory, typically over-relying on one modality at the expense of the other. HT-w/o-CFT demonstrates improvement by integrating real and synthetic data, but inadequately trains the model’s dependence on spatial memory during spatial revisit scenarios. Our Memory Forcing training approach achieves optimal performance by enabling the model to adaptively utilize temporal context when exploring new scenes while leveraging spatial memory when revisiting previously observed areas, effectively resolving the fundamental capability trade-off between generation quality and long-term memory retention.

**Retrieval Mechanism Comparison.** Our 3D-based approach substantially outperforms pose-based retrieval by leveraging explicit geometric representations for more precise identification of spatially relevant historical frames, while achieving superior computational efficiency as shown in Table 2.

## 5 CONCLUSIONS

We introduced Memory Forcing, a novel framework that addresses the fundamental trade-off between long-term spatial memory and new scene generation in autoregressive video models. Our approach consists of two key innovations: an efficient Geometry-indexed Spatial Memory that achieves constant-time retrieval complexity through streaming 3D reconstruction and point-to-frame retrieval, and a hybrid training strategy featuring Chained Forward Training that teaches models to dynamically balance temporal and spatial memory utilization. Our framework encourages adaptive contextual selection, relying on temporal memory for new scene generation while leveraging spatial memory for consistency in previously encountered areas. Extensive experiments demonstrate that Memory Forcing achieves superior performance in both spatial consistency and generative quality while maintaining computational efficiency for extended sequences, effectively resolving the capability trade-off that has limited prior memory-augmented video models.

486 **6 ETHICS STATEMENT**  
487488 We confirm that this research adheres to the ICLR Code of Ethics. We have carefully considered the  
489 ethical implications of our work and have strived to conduct our research with the highest standards  
490 of scientific integrity and responsibility. We outline the specific considerations below.  
491492 **1. Broader Impact and Potential for Harm**  
493494 This research aims to build more capable AI agents for simulated environments, such as games  
495 and robotics, by enhancing their long-term memory. While video generation technologies pose  
496 a dual-use risk (e.g., deepfakes), our model’s application is confined to the non-photorealistic,  
497 domain-specific world of Minecraft. This focus significantly mitigates the potential for misuse  
498 in creating malicious real-world synthetic media.499 **2. Data and Privacy**  
500501 Our research utilizes established public datasets (VPT, WorldMem) and a new benchmark we  
502 generated using the MineDojo simulator. All data consists of anonymized Minecraft gameplay  
503 and contains no Personally Identifiable Information (PII). To promote reproducibility and further  
504 research, we commit to open-sourcing our generated dataset upon the paper’s acceptance.  
505506 **7 REPRODUCIBILITY STATEMENT**  
507508 To ensure the reproducibility of our results, we provide comprehensive details of our methodology,  
509 experimental setup, and resources. Our core framework, Memory Forcing, is described in Section 3,  
510 with specific architectural details in Section 3.2 and 3.4, and our Memory forcing training strat-  
511 egy in Section 3.3. The complete experimental setup, including implementation details, hardware  
512 (NVIDIA H100/H20 GPUs), and key hyperparameters, is detailed in Section 4.1. The datasets used,  
513 including public benchmarks (VPT, WorldMem) and our newly generated evaluation data, are also  
514 described in Section 4.1. We provide a full breakdown of our evaluation metrics and comparisons  
515 against baselines in Section 4.2. Furthermore, we commit to releasing our source code and the newly  
516 generated dataset upon acceptance of this paper.517 **REFERENCES**  
518519 Bowen Baker, Ilge Akkaya, Peter Zhokov, Joost Huizinga, Jie Tang, Adrien Ecoffet, Brandon  
520 Houghton, Raul Sampedro, and Jeff Clune. Video pretraining (vpt): Learning to act by watching  
521 unlabeled online videos. *Advances in Neural Information Processing Systems*, 2022.  
522  
523 Amir Bar, Gaoyue Zhou, Danny Tran, Trevor Darrell, and Yann LeCun. Navigation world models.  
524 In *Proceedings of the Computer Vision and Pattern Recognition Conference*, 2025.  
525  
526 Haoxuan Che, Xuanhua He, Quande Liu, Cheng Jin, and Hao Chen. Gamegen-x: Interactive open-  
527 world game video generation. In *The Thirteenth International Conference on Learning Represen-  
528 tations*, 2024.  
529  
530 Boyuan Chen, Diego Martí Monsó, Yilun Du, Max Simchowitz, Russ Tedrake, and Vincent Sitz-  
531 mann. Diffusion forcing: Next-token prediction meets full-sequence diffusion. *Advances in  
532 Neural Information Processing Systems*, 2024.  
533  
534 Taiye Chen, Xun Hu, Zihan Ding, and Chi Jin. Learning world models for interactive video genera-  
535 tion. *arXiv preprint arXiv:2505.21996*, 2025.  
536  
537 Xinle Cheng, Tianyu He, Jiayi Xu, Junliang Guo, Di He, and Jiang Bian. Playing with transformer  
538 at 30+ fps via next-frame diffusion. *arXiv preprint arXiv:2506.01380*, 2025.  
539  
540 Etched Decart, Quinn McIntyre, Spruce Campbell, Xinlei Chen, and Robert Wachen. Oasis: A  
541 universe in a transformer. *URL: https://oasis-model.github.io*, 2024.  
542  
543 Prafulla Dhariwal and Alexander Nichol. Diffusion models beat gans on image synthesis. *Advances  
544 in neural information processing systems*, 2021.

540 Linxi Fan, Guanzhi Wang, Yunfan Jiang, Ajay Mandlekar, Yuncong Yang, Haoyi Zhu, Andrew  
 541 Tang, De-An Huang, Yuke Zhu, and Anima Anandkumar. Minedojo: Building open-ended em-  
 542 bodied agents with internet-scale knowledge. In *Thirty-sixth Conference on Neural Information  
 543 Processing Systems Datasets and Benchmarks Track*, 2022. URL [https://openreview.net/forum?id=rc8o\\_j8I8PX](https://openreview.net/forum?id=rc8o_j8I8PX).

545 Ruili Feng, Han Zhang, Zhantao Yang, Jie Xiao, Zhilei Shu, Zhiheng Liu, Andy Zheng, Yukun  
 546 Huang, Yu Liu, and Hongyang Zhang. The matrix: Infinite-horizon world generation with real-  
 547 time moving control. *arXiv preprint arXiv:2412.03568*, 2024.

549 Junliang Guo, Yang Ye, Tianyu He, Haoyu Wu, Yushu Jiang, Tim Pearce, and Jiang Bian.  
 550 Mineworld: a real-time and open-source interactive world model on minecraft. *arXiv preprint  
 551 arXiv:2504.08388*, 2025.

552 William H Guss, Brandon Houghton, Nicholay Topin, Phillip Wang, Cayden Codel, Manuela  
 553 Veloso, and Ruslan Salakhutdinov. Minerl: A large-scale dataset of minecraft demonstrations.  
 554 *arXiv preprint arXiv:1907.13440*, 2019.

555 David Ha and Jürgen Schmidhuber. Recurrent world models facilitate policy evolution. *Advances  
 556 in neural information processing systems*, 2018a.

558 David Ha and Jürgen Schmidhuber. World models. *arXiv preprint arXiv:1803.10122*, 2018b.

560 Danijar Hafner, Timothy Lillicrap, Jimmy Ba, and Mohammad Norouzi. Dream to control: Learning  
 561 behaviors by latent imagination. *arXiv preprint arXiv:1912.01603*, 2019.

562 Danijar Hafner, Timothy Lillicrap, Mohammad Norouzi, and Jimmy Ba. Mastering atari with dis-  
 563 crete world models. *arXiv preprint arXiv:2010.02193*, 2020.

565 William Harvey, Saeid Naderiparizi, Vaden Masrani, Christian Weilbach, and Frank Wood. Flexible  
 566 diffusion modeling of long videos. *Advances in neural information processing systems*, 2022.

567 Xianglong He, Chunli Peng, Zexiang Liu, Boyang Wang, Yifan Zhang, Qi Cui, Fei Kang, Biao  
 568 Jiang, Mengyin An, Yangyang Ren, et al. Matrix-game 2.0: An open-source, real-time, and  
 569 streaming interactive world model. *arXiv preprint arXiv:2508.13009*, 2025.

571 Roberto Henschel, Levon Khachatryan, Hayk Poghosyan, Daniil Hayrapetyan, Vahram Tadevosyan,  
 572 Zhangyang Wang, Shant Navasardyan, and Humphrey Shi. Streamingt2v: Consistent, dynamic,  
 573 and extendable long video generation from text. In *Proceedings of the Computer Vision and  
 574 Pattern Recognition Conference*, 2025.

575 Jonathan Ho, AjayN. Jain, and Pieter Abbeel. Denoising diffusion probabilistic models. *Advances  
 576 in neural information processing systems*, 2020.

577 Yining Hong, Beide Liu, Maxine Wu, Yuanhao Zhai, Kai-Wei Chang, Linjie Li, Kevin Lin, Chung-  
 578 Ching Lin, Jianfeng Wang, Zhengyuan Yang, et al. Slowfast-vgen: Slow-fast learning for action-  
 579 driven long video generation. *arXiv preprint arXiv:2410.23277*, 2024.

581 Xun Huang, Zhengqi Li, Guande He, Mingyuan Zhou, and Eli Shechtman. Self forcing: Bridging  
 582 the train-test gap in autoregressive video diffusion. *arXiv preprint arXiv:2506.08009*, 2025.

583 Dan Kondratyuk, Lijun Yu, Xiuye Gu, José Lezama, Jonathan Huang, Grant Schindler, Rachel  
 584 Hornung, Vighnesh Birodkar, Jimmy Yan, Ming-Chang Chiu, et al. Videopoet: A large language  
 585 model for zero-shot video generation. *arXiv preprint arXiv:2312.14125*, 2023.

587 Runjia Li, Philip Torr, Andrea Vedaldi, and Tomas Jakab. Vmem: Consistent interactive video scene  
 588 generation with surfel-indexed view memory. *arXiv preprint arXiv:2506.18903*, 2025a.

589 Zongyi Li, Shujie Hu, Shujie Liu, Long Zhou, Jeongsoo Choi, Lingwei Meng, Xun Guo, Jinyu Li,  
 590 Hefei Ling, and Furu Wei. Arlon: Boosting diffusion transformers with autoregressive models  
 591 for long video generation. In *ICLR*, 2025b.

593 Dominic Maggio, Hyungtae Lim, and Luca Carlone. Vggt-slam: Dense rgb slam optimized on the  
 sl (4) manifold. *arXiv preprint arXiv:2505.12549*, 2025.

594 OpenAI. Video generation models as world simulators, 2024.  
 595

596 J Parker-Holder, P Ball, J Bruce, V Dasagi, K Holsheimer, C Kaplanis, A Moufarek, G Scully,  
 597 J Shar, J Shi, et al. Genie 2: A large-scale foundation world model. *URL: https://deepmind.  
 598 google/discover/blog/genie-2-a-large-scale-foundation-world-model*, 2024.

599 William Peebles and Saining Xie. Scalable diffusion models with transformers. In *Proceedings of  
 600 the IEEE/CVF international conference on computer vision*, 2023.  
 601

602 Ryan Po, Yotam Nitzan, Richard Zhang, Berlin Chen, Tri Dao, Eli Shechtman, Gordon Wetzstein,  
 603 and Xun Huang. Long-context state-space video world models. *arXiv preprint arXiv:2505.20171*,  
 604 2025.

605 Kiwhan Song, Boyuan Chen, Max Simchowitz, Yilun Du, Russ Tedrake, and Vincent Sitzmann.  
 606 History-guided video diffusion. *arXiv preprint arXiv:2502.06764*, 2025.  
 607

608 Hansi Teng, Hongyu Jia, Lei Sun, Lingzhi Li, Maolin Li, Mingqiu Tang, Shuai Han, Tianning  
 609 Zhang, WQ Zhang, Weifeng Luo, et al. Magi-1: Autoregressive video generation at scale. *arXiv  
 610 preprint arXiv:2505.13211*, 2025.

611 Dani Valevski, Yaniv Leviathan, Moab Arar, and Shlomi Fruchter. Diffusion models are real-time  
 612 game engines. In *The Thirteenth International Conference on Learning Representations*, 2024.  
 613

614 Vikram Voleti, Alexia Jolicoeur-Martineau, and Chris Pal. Mcvd-masked conditional video diffusion  
 615 for prediction, generation, and interpolation. *Advances in neural information processing systems*,  
 616 2022.

617 Jianyuan Wang, Minghao Chen, Nikita Karaev, Andrea Vedaldi, Christian Rupprecht, and David  
 618 Novotny. Vggt: Visual geometry grounded transformer. In *Proceedings of the Computer Vision  
 619 and Pattern Recognition Conference*, 2025a.

620 Qianqian Wang, Yifei Zhang, Aleksander Holynski, Alexei A Efros, and Angjoo Kanazawa. Con-  
 621 tinuous 3d perception model with persistent state. In *Proceedings of the Computer Vision and  
 622 Pattern Recognition Conference*, 2025b.  
 623

624 Shuzhe Wang, Vincent Leroy, Yohann Cabon, Boris Chidlovskii, and Jerome Revaud. Dust3r: Ge-  
 625 ometric 3d vision made easy. In *Proceedings of the IEEE/CVF Conference on Computer Vision  
 626 and Pattern Recognition*, 2024.

627 Yifan Wang, Jianjun Zhou, Haoyi Zhu, Wenzheng Chang, Yang Zhou, Zizun Li, Junyi Chen, Jiang-  
 628 miao Pang, Chunhua Shen, and Tong He. pi3: Scalable permutation-equivariant visual geometry  
 629 learning. *arXiv preprint arXiv:2507.13347*, 2025c.

630 Jialong Wu, Shaofeng Yin, Ningya Feng, Xu He, Dong Li, Jianye Hao, and Mingsheng Long.  
 631 ivideogpt: Interactive videogpts are scalable world models. *Advances in Neural Information  
 632 Processing Systems*, 2024.  
 633

634 Yuqi Wu, Wenzhao Zheng, Jie Zhou, and Jiwen Lu. Point3r: Streaming 3d reconstruction with  
 635 explicit spatial pointer memory. *arXiv preprint arXiv:2507.02863*, 2025.

636 Zeqi Xiao, Yushi Lan, Yifan Zhou, Wenqi Ouyang, Shuai Yang, Yanhong Zeng, and Xin-  
 637 gang Pan. Worldmem: Long-term consistent world simulation with memory. *arXiv preprint  
 638 arXiv:2504.12369*, 2025.  
 639

640 Desai Xie, Zhan Xu, Yicong Hong, Hao Tan, Difan Liu, Feng Liu, Arie Kaufman, and Yang Zhou.  
 641 Progressive autoregressive video diffusion models. In *Proceedings of the Computer Vision and  
 642 Pattern Recognition Conference*, 2025.

643 Wilson Yan, Danijar Hafner, Stephen James, and Pieter Abbeel. Temporally consistent transformers  
 644 for video generation. In *International Conference on Machine Learning*. PMLR, 2023.  
 645

646 Jianing Yang, Alexander Sax, Kevin J Liang, Mikael Henaff, Hao Tang, Ang Cao, Joyce Chai,  
 647 Franziska Meier, and Matt Feiszli. Fast3r: Towards 3d reconstruction of 1000+ images in one  
 forward pass. In *Proceedings of the Computer Vision and Pattern Recognition Conference*, 2025.

648 Jiwen Yu, Jianhong Bai, Yiran Qin, Quande Liu, Xintao Wang, Pengfei Wan, Di Zhang, and Xi-  
 649 hui Liu. Context as memory: Scene-consistent interactive long video generation with memory  
 650 retrieval. *arXiv preprint arXiv:2506.03141*, 2025a.

651  
 652 Jiwen Yu, Yiran Qin, Xintao Wang, Pengfei Wan, Di Zhang, and Xihui Liu. Gamefactory: Creating  
 653 new games with generative interactive videos. *arXiv preprint arXiv:2501.08325*, 2025b.

654 Yifan Zhang, Chunli Peng, Boyang Wang, Puyi Wang, Qingcheng Zhu, Fei Kang, Biao Jiang, Ze-  
 655 dong Gao, Eric Li, Yang Liu, et al. Matrix-game: Interactive world foundation model. *arXiv*  
 656 *preprint arXiv:2506.18701*, 2025.

## 658 A APPENDIX

### 660 A.1 DECLARATION OF LLM USAGE

662 Large Language Models (LLMs) were used as general-purpose assistive tools to improve the grammar and clarity of this manuscript. The core scientific contributions, including the methodology, experimental design, and analysis, are entirely our own. The authors have reviewed all text and take full responsibility for the content of this paper.

### 667 A.2 CHAINED FORWARD TRAINING ALGORITHM

---

#### 670 Algorithm 1 Chained Forward Training (CFT)

---

671 **Require:** Video  $\mathbf{x}$ , conditioning inputs  $\mathcal{C}$ , forward steps  $T$ , window size  $W$ , model  $\epsilon_\theta$   
 672 1: Initialize  $\mathcal{F}_{\text{pred}} \leftarrow \emptyset$ ,  $\mathcal{L}_{\text{total}} \leftarrow 0$   
 673 2: **for**  $j = 0$  **to**  $T - 1$  **do**  
 674 3: Construct window  $\mathcal{W}_j[k] \leftarrow \mathcal{F}_{\text{pred}}[k]$  if  $k \in \mathcal{F}_{\text{pred}}$  else  $\mathbf{x}_k$  for  $k \in [j, j + W - 1]$   
 675 4: Compute  $\mathcal{L}_j \leftarrow \|\epsilon - \epsilon_\theta(\mathcal{W}_j, \mathcal{C}_j, t)\|^2$ , update  $\mathcal{L}_{\text{total}} \leftarrow \mathcal{L}_{\text{total}} + \mathcal{L}_j$   
 676 5: If  $j < T - 1$ :  $\mathcal{F}_{\text{pred}}[j + W - 1] \leftarrow \hat{\mathbf{x}}_{j + W - 1}$  {Fewer denoising steps}  
 677 6: **end for**  
 678 7: **return**  $\mathcal{L}_{\text{chain}} \leftarrow \mathcal{L}_{\text{total}}/T$

---

### 680 A.3 DATASET DETAILS

681 We utilize the WorldMem (Xiao et al., 2025) dataset together with three additional datasets col-  
 682 lected using MineDojo (Fan et al., 2022) to evaluate our model across multiple dimensions: mem-  
 683 ory capacity, generalization abilities, scene exploration, and efficiency. The WorldMem (Xiao et al.,  
 684 2025) dataset contains 150 video sequences of 1,500 frames each, sampled from five terrain types:  
 685 *ice\_plains*, *desert*, *savanna*, *sunflower\_plains*, and *plains*. The Scene Generation dataset includes  
 686 300 sequences of 800 frames each, while the Efficiency dataset consists of 20 sequences of 4,000  
 687 frames. The Generalization Abilities dataset comprises 150 sequences of 800 frames each, sam-  
 688 pled from nine unseen terrains: *extreme\_hills*, *taiga*, *stone\_beach*, *swampland*, *river*, *beach*, *mesa*,  
 689 *frozen\_ocean*, and *forest\_hills*. Dataset statistics are summarized in Table 4.

690 For action configurations, all MineDojo-collected datasets adopt the same setup as WorldMem, in-  
 691 cluding movement actions (*left*, *right*, *forward*, *back*) and view-control actions (*look\_up*, *look\_down*,  
 692 *turn\_left*, *turn\_right*). The Memory Capabilities dataset constrains agents within confined re-  
 693 gions with diverse actions including vertical movement. For Scene Generation and Generalization  
 694 datasets, we use a two-phase strategy: initial 600 frames with full action diversity, followed by  
 695 restricted actions (*forward*, *turn\_left*, *turn\_right*) to assess generation capabilities.

### 698 A.4 MODEL COMPARISON

700 Table 5 provides a comprehensive comparison of our approach with existing video generation mod-  
 701 els for Minecraft environments, highlighting key differences in memory mechanisms, storage effi-  
 702 ciency, and capabilities across different methodological paradigms.

702  
703  
704 Table 4: Dataset statistics for model evaluation.  
705  
706  
707  
708  
709

Dataset	Video Count	Frames per Video	Terrain Types
Efficiency	20	4,000	5
Generation Performance	300	800	5
Generalization Performance	150	800	9
Long-term Memory	150	1,500	5

710  
711 Table 5: Comparison of Video Generation Models on Minecraft  
712

Method	Memory Type (Complexity)	Memory Storage	Memory Scope	Dataset	Size	Video Length	Actions
Oasis	/	/	/	VPT	2.5M	64 frames	25
Mineworld	/	/	/	VPT	2.5M	64 frames	25
NFD	/	/	/	VPT	2.5M	64 frames	25
LSVM	State Space Model (O(1))	Compressed hidden state	Limited by training length	TECO (Yan et al., 2023)	200K	150 frames	4
VRAG	Similarity-based RAG (O(1))	Fixed-length buffer	Limited by buffer size	MineRL (Guss et al., 2019)	1K	1200 frames	5
Worldmem	Pose-based RAG (O(n))	Memory bank (Stores all frames)	Long-term	MineDojo	20K	1500 frames	8
Ours	3D-based RAG (O(1))	Scene-dependent sparse storage	Long-term	VPT+MineDojo	85K	1500 frames	25

721 The first group represents traditional autoregressive video models without explicit memory mech-  
722 anisms. Models like Oasis (Decart et al., 2024), Mineworld (Guo et al., 2025), and NFD (Cheng  
723 et al., 2025) rely solely on temporal context windows and demonstrate strong performance in scene  
724 generation but suffer from spatial inconsistency when revisiting previously encountered areas due to  
725 their limited memory scope.

726 The second group encompasses recent memory-augmented approaches that attempt to extend model  
727 capabilities through various memory mechanisms. LSVM (Po et al., 2025) employs state space  
728 models to compress historical information into hidden states, achieving constant-time complexity  
729 but with memory scope fundamentally limited by training sequence length. VRAG (Chen et al.,  
730 2025) utilizes similarity-based retrieval with fixed-length buffers, providing constant-time access but  
731 constraining long-term memory capacity. WorldMem implements pose-based retrieval with com-  
732 prehensive frame storage, enabling true long-term memory but suffering from linear complexity growth  
733 as memory banks accumulate redundant information during extended sequences.

734 Our Memory Forcing framework uniquely combines the advantages of both paradigms while ad-  
735 dressing their respective limitations. Unlike traditional models, we maintain long-term spatial mem-  
736 ory through explicit 3D scene representation. Unlike existing memory-augmented approaches, our  
737 3D-based retrieval system achieves constant-time complexity with scene-dependent sparse storage  
738 that adapts to spatial redundancy patterns. This design enables efficient scaling to extended se-  
739 quences while preserving both spatial consistency and scene generation capabilities across the most  
740 comprehensive action space among compared methods.

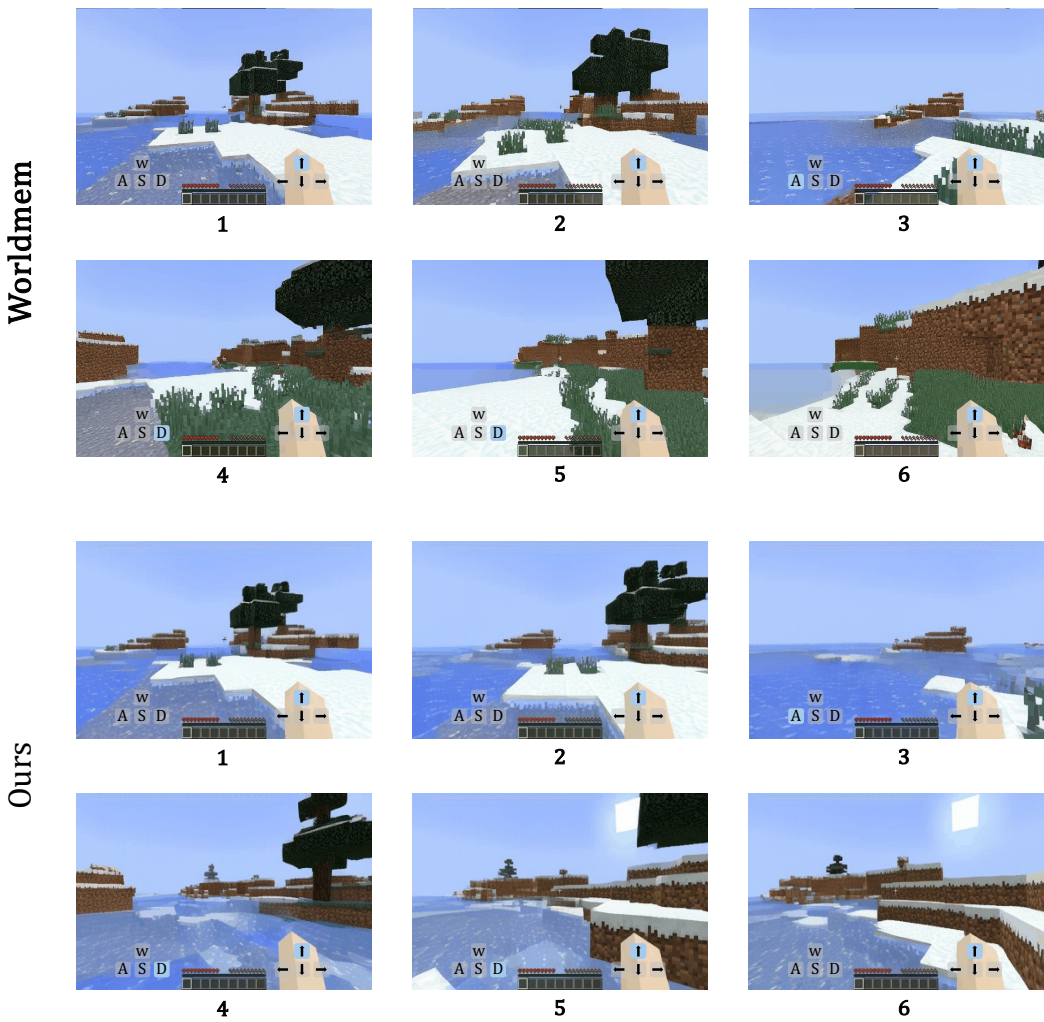
## 741 742 A.5 LIMITATIONS AND FUTURE WORK.

743  
744 **Limitations.** While Memory Forcing demonstrates strong performance in memory retention and  
745 generation quality, several limitations remain. Our current implementation is primarily validated  
746 on Minecraft gameplay scenarios, which may not directly generalize to other environments without  
747 domain-specific adaptation. Additionally, our model operates at a fixed resolution of  $384 \times 224$   
748 pixels, which may limit visual detail in applications requiring higher fidelity.

749  
750 **Future Work.** Future research should focus on extending our framework to diverse gaming en-  
751 vironments and real-world scenarios at higher resolutions. We plan to explore domain adaptation  
752 techniques that preserve core memory mechanisms while accommodating different visual char-  
753 acteristics. Additionally, investigating simplified architectural designs that maintain memory advantages  
754 while reducing implementation complexity could enhance broader applicability. Integration with ad-  
755 vanced acceleration techniques may further improve both efficiency and performance across diverse  
interactive scenarios.

756 A.6 ADDITIONAL QUALITATIVE COMPARISONS  
757

758 We present additional qualitative analyses of different models' performance in novel scene gen-  
759 eration. Across Figures 6–8, our method shows superior spatial coherence, temporal continuity,  
760 and scene detail compared to baseline models in both familiar and unfamiliar terrains. Figure 5  
761 demonstrates generalization on frozen ocean terrain. While WorldMem reproduces familiar training  
762 terrains like plains, our model successfully maintains the target frozen ocean environment, showing  
763 better generalization capabilities. Figures 6 and 7 compare performance across extreme hills, ice  
764 plains, and desert terrains. Baseline methods (Oasis, NFD, WorldMem) often generate unrealistic  
765 views, violate spatial consistency, or fail to reflect agent motion. Our approach maintains geometric  
766 and temporal coherence while producing high-quality novel scenes. Figure 8 examines long-term  
767 memory scenarios. Specialized long-term memory models struggle with novel scene generation and  
768 show limited generalization in new environments. Our model effectively uses long-term memory to  
769 generate consistent, realistic scenes while preserving spatial and temporal coherence. These com-  
770 parisons demonstrate that our geometry-indexed spatial memory and generative approach delivers  
771 robust performance across diverse terrains, generalization tasks, and long-term memory scenarios,  
772 outperforming existing baselines.



805 Figure 5: Generalization performance on frozen ocean. When generating frozen ocean terrain,  
806 WorldMem (Xiao et al., 2025) produces novel scenes resembling the plains terrain from the training  
807 set. By contrast, our model preserves the frozen ocean terrain across novel scene generations.  
808  
809

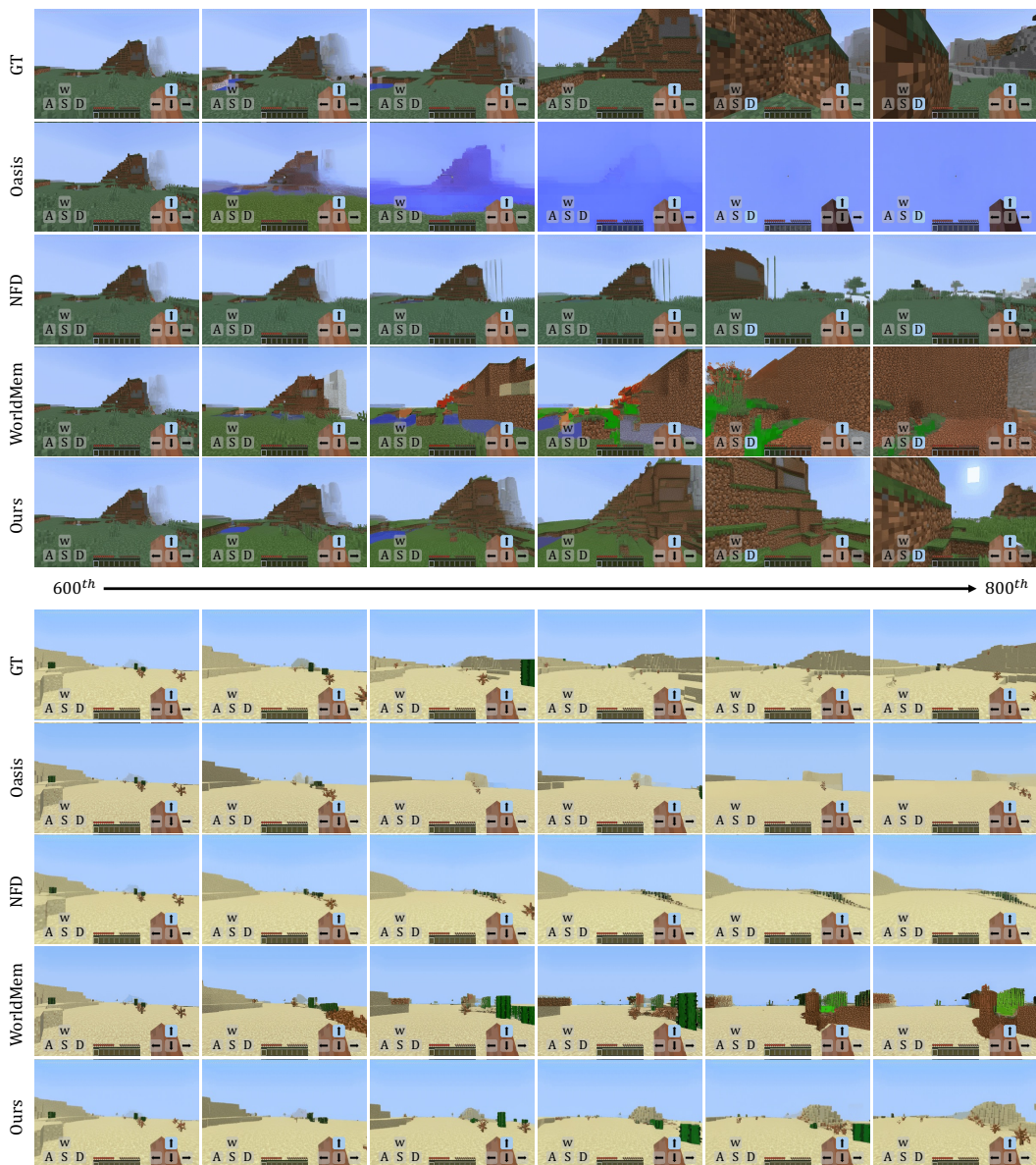


Figure 6: Qualitative results. Comparison of different models' novel scene generation on two terrains: extreme hills (top) and desert (bottom). In extreme hills, our method generates novel views while preserving spatial consistency, whereas Oasis (Decart et al., 2024) fails, collapsing to blue images. WorldMem (Xiao et al., 2025) and NFD (Cheng et al., 2025) produce unrealistic views that break spatial consistency. In desert, Oasis (Decart et al., 2024) and NFD (Cheng et al., 2025) fail to reflect the agent's forward motion, and WorldMem (Xiao et al., 2025) lacks temporal and spatial consistency. By contrast, our method maintains spatial coherence and produces rich, realistic novel views.

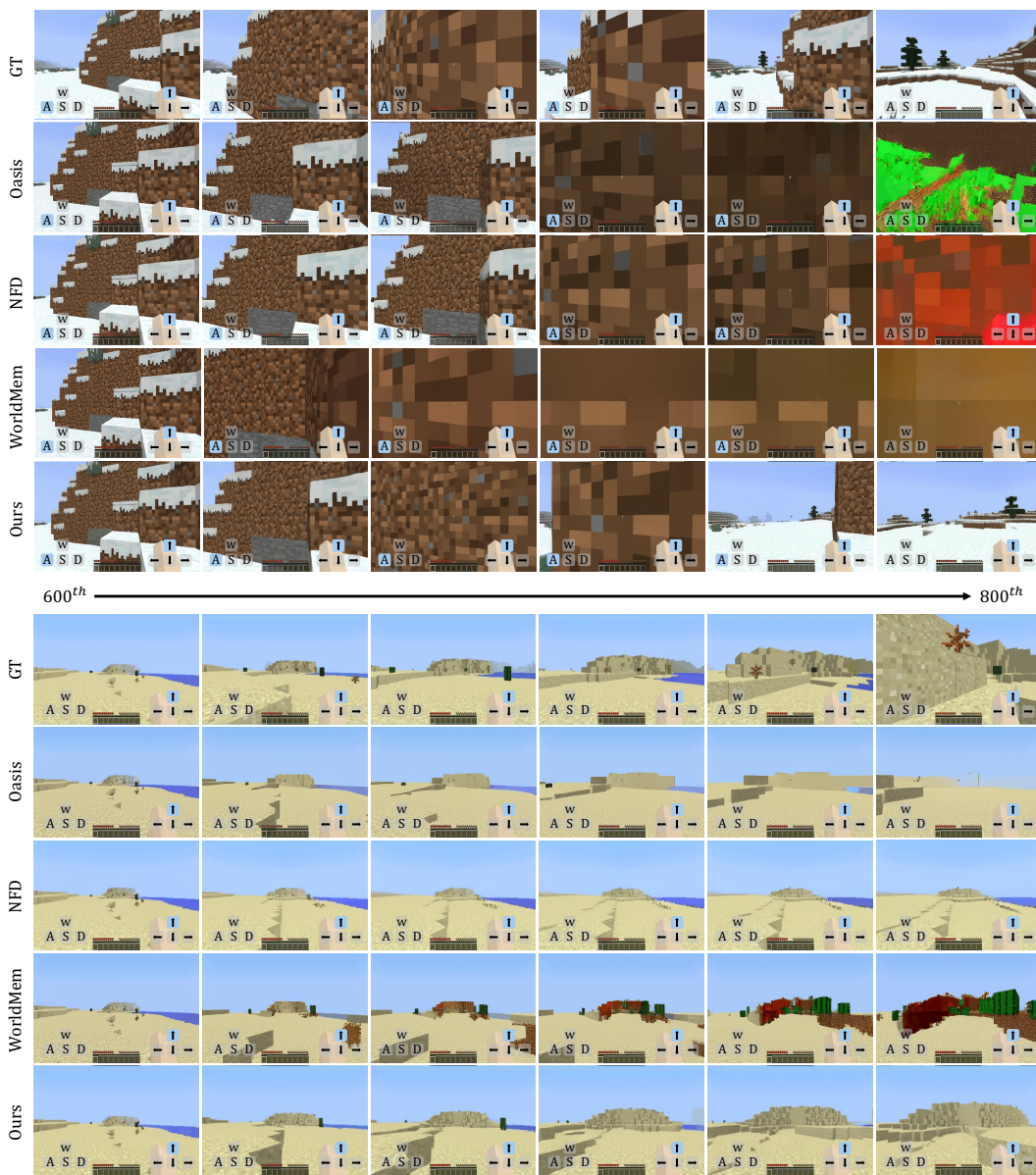


Figure 7: Qualitative results. Comparison of different models’ novel scene generation on two terrains: ice plains (top) and desert (bottom). In the ice plains scenario, an action sequence drives the agent into a confined area, testing the models’ memory in generating novel scenes. Oasis (Decart et al., 2024), NFD (Cheng et al., 2025), and WorldMem (Xiao et al., 2025) fail to produce correct views when the agent turns left and moves forward, remaining trapped. By contrast, our model successfully generates novel views after escaping while preserving the ice plains terrain. In the desert scenario, NFD (Cheng et al., 2025) fails to reflect the agent’s forward motion, while WorldMem (Xiao et al., 2025) and Oasis (Decart et al., 2024) violate temporal and spatial consistency. Our method consistently maintains spatial coherence and generates realistic novel views.

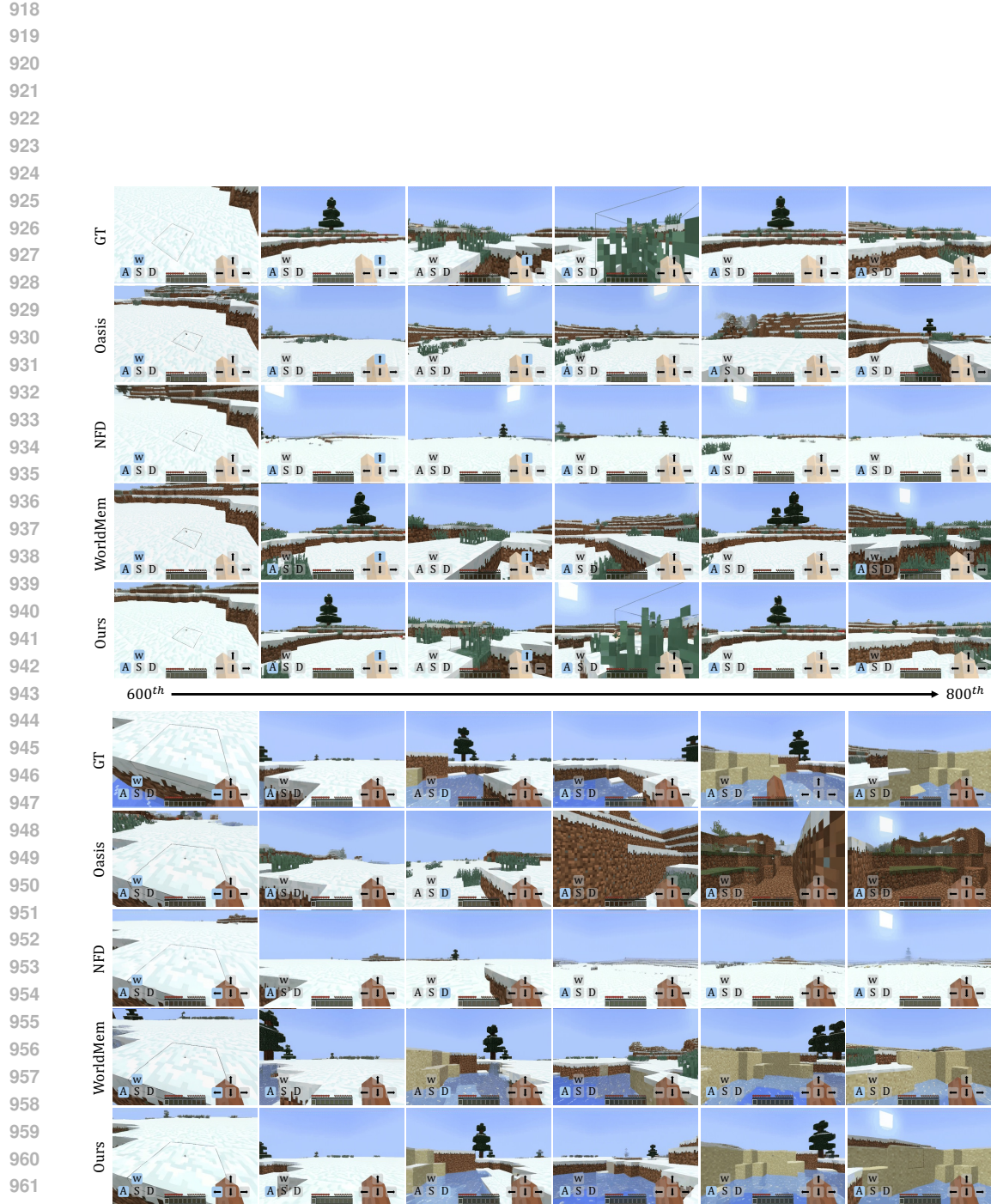


Figure 8: Qualitative results on long-term memory across different models. We compare the generative capabilities of different models under long-term memory settings. Our model achieves the best spatial consistency, temporal continuity, and preserves rich scene details.